Inorg. Chem. **2005**, *44*, 9497–9505

Spectroscopic and Electrochemical Studies of U(IV)–Hexachloro Complexes in Hydrophobic Room-Temperature Ionic Liquids [BuMeIm][Tf_2N] and [$MeBu_3N$][Tf_2N]

S. I. Nikitenko,[†] C. Cannes,[‡] C. Le Naour,*[,‡] P. Moisy,[§] and D. Trubert[‡]

Institute of Physical Chemistry, Russian Academy of Science, Leninskii Pr. 31, 117915 Moscow, Russia, Institut de Physique Nucléaire, Radiochimie, CNRS-IN2P3-UPS, BP1-91406 Orsay Cedex, France, and Commissariat à l'Energie Atomique, Valrhô/Marcoule, DEN/DRCP/SCPS, Bât. 399, BP 17171, 30207 Bagnols-sur-Cèze, France

Received June 28, 2005

The behavior of U(IV) octahedral complexes [cation]$_2$[UCl_6], where the [cation]$^+$ is [BuMeIm]$^+$ and [$MeBu_3N$]$^+$, is studied using UV/visible spectroscopy, cyclic staircase voltammetry, and rotating disk electrode voltammetry in hydrophobic room-temperature ionic liquids (RTILs) [BuMeIm][Tf_2N] and [$MeBu_3N$][Tf_2N], where BuMeIm$^+$ and $MeBu_3N^+$ are 1-butyl-3-methylimidazolium and tri-*n*-butylmethylammonium cations, respectively, and Tf_2N^- is the bis-(trifluoromethylsulfonyl)imide anion. The absorption spectra of [cation]$_2$[UCl_6] complexes in the RTIL solutions are similar to the diffuse solid-state reflectance spectra of the corresponding solid species, indicating that the octahedral complex UCl_6^{2-} is the predominant chemical form of U(IV) in Tf_2N^--based hydrophobic ionic liquids. Hexachloro complexes of U(IV) are stable to hydrolysis in the studied RTILs. Voltammograms of UCl_6^{2-} at the glassy carbon electrode in both RTILs and at the potential range of –2.5 to +1.0 V versus Ag/Ag(I) reveal the following electrochemical couples: UCl_6^-/UCl_6^{2-} (quasi-reversible system), UCl_6^{2-}/UCl_6^{3-} (quasi-reversible system), and $UCl_6^{2-}/UCl_6(Tf_2N)_x^{-(3+x)}$ (irreversible reduction). The voltammetric half-wave potential, $E_{p/2}$, of the U(V)/U(IV) couple in [BuMeIm][Tf_2N] is positively shifted by 80 mV compared with that in [$MeBu_3N$][Tf_2N]. The positive shift in the $E_{p/2}$ value for the quasi-reversible U(IV)/U(III) couple is much greater (250 mV) in [BuMeIm][Tf_2N]. Presumably, the potential shift is due to the specific interaction of BuMeIm$^+$ with the uranium–hexachloro complex in ionic liquid. Scanning the negative potential to –3.5 V in [$MeBu_3N$][Tf_2N] solutions of UCl_6^{2-} reveals the presence of an irreversible cathodic process at the peak potential equal to –3.12 V (at 100 mV/s and 60 °C), which could be attributed to the reduction of U(III) to U(0).

Introduction

Room-temperature ionic liquids (RTILs) are new and remarkable solvents that can be defined as salts with a melting point below 100 °C. They are composed of a bulk organic cation (alkylimidazolium, alkylpyridinium, tetraalkylammonium, etc.) and various inorganic anions [Cl^-, $AlCl_4^-$, PF_6^-, $CF_3SO_3^-$, $(CF_3SO_2)_2N^-$, etc.], and their properties can be tailored by a suitable choice of the cation/anion combination.[1] Ionic liquids offer a unique opportunity to study the fundamental chemistry of actinides without interference from hydrolysis. In principle, their use would allow the creation of the next generation of actinide separation and purification processes capable of reducing the volume of radioactive waste and improving the safety of spent nuclear fuel reprocessing.[2–6]

* To whom correspondence should be addressed. E-mail: lenaour@ipno.in2p3.fr.
[†] RAS.
[‡] Institut de Physique Nucléaire.
[§] CEA.

(1) *Ionic Liquids in Synthesis*; Wasserscheid, P., Welton, T., Eds.; Wiley: Weinheim, Germany, 2003.
(2) Thied, R. C.; Hatter, J. E.; Seddon, K. R.; Pitner, W. R.; Rooney, D. W.; Hebditch, D. World Patent WO01/13379A1, August 18, 1999.
(3) (a) Oldham, W. J.; Costa, D. A.; Smith, W. H. Development of Room-Temperature Ionic Liquids for Applications in Actinide Chemistry. In *Ionic Liquids. Industrial Applications to Green Chemistry*; Rogers, R. D., Seddon, K. R., Eds.; ACS Symposium Series, 818; American Chemical Society: Washington, DC, 2002; p 188. (b) Mudring, A.-V.; Babai, A.; Arenz, S.; Giernoth, R. *Angew. Chem., Int. Ed.* **2005**, *44*, 5485.
(4) Visser, A. E.; Rogers, R. D. *J. Solid State Chem.* **2003**, *171*, 109.
(5) Dai, S.; Ju, Y. H.; Barnes, C. E. *J. Chem. Soc., Dalton Trans.* **1999**, 1201.

10.1021/ic051065b CCC: $30.25
Published on Web 11/12/2005

Most studies of actinide behavior in ionic liquids are focused on spectroscopic and electrochemical investigations of actinides in chloroaluminate-based ionic liquids.[7−16] Nevertheless, these RTILs are extremely water-sensitive and ill-suited for use in radiochemistry. Moreover, most of the studies have been done in basic ionic liquids, that is, in excess of chloride ions. The electrochemical window is thus anodically limited by the oxidation of the chloride ions. For example, the U(V)/U(IV) system cannot be observed in such media. Hydrophobic ionic liquids with the bis(trifluoromethylsulfonyl)imide anion (Tf_2N^-) are of particular interest as a result of their water stability, relatively low viscosity, high conductivity, and good electrochemical and thermal stability. In contrast to $AlCl_4^-$, the anion Tf_2N^- may act as a coordinating ligand, which, in principle, is able to form complexes with actinides.[3] Information about actinide chemistry in water-stable RTILs is relatively scarce, and the fundamental knowledge about the actinide chemistry in these solvents is indispensable for any future processes in the nuclear fuel cycle, including actinide electrorefining and solvent extraction. Studies of UO_2^{2+} extracted from nitric acid solutions with octyl(phenyl)-*N*,*N*-diisobutylcarbamoylmethyl phosphine oxide in Tf_2N^--based ionic liquids gave no evidence of Tf_2N^- coordination with uranyl.[4] On the contrary, it has been shown that Tf_2N^- can be coordinated to UO_2^{2+} and U(IV) in solutions of $[Me_3BuN][Tf_2N]$, where Me_3BuN^+ is the trimethyl-*n*-butylammonium cation, in the absence of other strong ligands.[17,18] Electrochemical reduction of hydrated $U(Tf_2N)_4 \cdot xH_2O$ in $[Me_3BuN][Tf_2N]$ has shown several cathodic processes, probably related to different U(IV) complexes in RTIL.[18] It has also been reported that Np(IV) is oxidized spontaneously to NpO_2^+ in solutions of hydrated complexes of $Np(Tf_2N)_4 \cdot xH_2O$ in $[Me_3BuN][Tf_2N]$.[18] The dissolution of $[BuMeIm]_2[AnCl_6]$, where $BuMeIm^+$ is 1-butyl-3-methylimidazolium and An(IV) is Np(IV) or Pu(IV), in $[BuMeIm][Tf_2N]$ has yielded solutions of octahedral complexes of $AnCl_6^{2-}$.[19] Adding [BuMeIm]Cl to these solutions produces nonoctahedral An(IV) chloride complexes with a Cl^-/An(IV) ratio higher than 6:1.[19]

This paper reports spectroscopic and electrochemical studies of $[BuMeIm]_2[UCl_6]$ and $[MeBu_3N]_2[UCl_6]$ in $[BuMeIm][Tf_2N]$ and $[MeBu_3N][Tf_2N]$ RTILs, respectively. First, the work is focused on the determination of the predominant chemical forms of U(IV) in both ionic liquids and its stability toward hydrolysis. Second, the uranium redox potentials are determined and compared in $[BuMeIm][Tf_2N]$ and in $[MeBu_3N][Tf_2N]$ to study the solvation of these chloro−uranium complexes.

Experimental Section

Chemicals and Synthesis. Ionic liquids $[BuMeIm][Tf_2N]$ and $[MeBu_3N][Tf_2N]$ were prepared by metathesis reactions from [BuMeIm]Cl and $[MeBu_3N][OH]$, respectively, with HTf_2N in an aqueous medium. [BuMeIm]Cl was synthesized by quaternization of 1-methylimidazole by 1-chlorobutane and washed with ethyl acetate, as described recently.[1] Other chemicals (Aldrich, highest purity) were used in the synthesis without additional purification. The as-prepared RTILs were washed with deionized water (18 MΩ·cm) to a neutral reaction. In the case of $[BuMeIm][Tf_2N]$, the absence of chloride ions was controlled by a $AgNO_3$ test of the aqueous phase pre-equilibrated with a RTIL. Organic impurities were removed from the ionic liquids with activated carbon for 12 h, after which the mixtures were passed through a column with small amounts of acidic alumina. ^1H NMR analysis revealed the absence (<1%) of residual reagents in the purified ionic liquids. The RTILs were dried overnight under reduced pressure (∼5 mbar) at 70−80 °C. The water concentrations in the dried RTILs, measured by coulometric Karl−Fisher titration, were found equal to 125 ± 20 ppm for $[BuMeIm][Tf_2N]$ and 174 ± 30 ppm for $[MeBu_3N][Tf_2N]$.

$[Cation]_2[UCl_6]$ complexes, where $cation^+$ is $BuMeIm^+$ or $MeBu_3N^+$, were prepared by precipitation from U(IV) solutions in 10 M HCl in the presence of a slight excess of the corresponding [cation]Cl. The precipitates were washed with cold acetone, saturated with argon, and dried under reduced pressure at room temperature. The initial U(IV) solutions were prepared by the dissolution of uranium metal in concentrated HCl. All uranium(IV) solid complexes, their solutions, and the samples for spectroscopic and voltammetric measurements were prepared and stored in an argon-filled drybox. Both complexes are well-soluble in studied RTILs. In the preliminary experiments it was shown that 0.05 M UCl_6^{2-} solutions can be easily prepared under gentle heating.

Spectroscopic and Electrochemical Devices. The absorption spectra were recorded with a Shimadzu UV-2501 PC spectrophotometer using 1-cm path length quartz cells that were sealed airtight by Teflon stoppers. The diffuse solid-state reflectance spectra were measured with a U-3000 Hitachi device equipped with a 60-mm diameter integrating sphere.

The voltammetric study was carried out with an Autolab PGSTAT30 device without an ohmic drop compensation. A three-electrode thermostated Pyrex commercial electrochemical cell (V = 4 mL) was used with a glassy carbon (GC) disk working electrode (d = 3 mm, from Radiometer), Ag/Ag(I) reference electrode, and Pt counter electrode. The reference electrode was

(6) Dietz, M. L.; Dzielawa, J. A. *Chem. Commun.* **2001**, 2124.
(7) De Waele, R.; Heerman, L.; D'Olieslager, W. *J. Electroanal. Chem.* **1982**, *142*, 137.
(8) Hitchcock, P. B.; Mohammed, T. J.; Seddon, K. R.; Zora, J. A.; Hussey, C. L.; Ward, E. H. *Inorg. Chim. Acta* **1986**, *113*, L25.
(9) Anderson, C. J.; Deakin, M. R.; Choppin, G. R.; D'Olieslager, W.; Heerman, L.; Pruett, D. J. *Inorg. Chem.* **1991**, *30*, 4013.
(10) Sinha, S. P. *Lanthanide Actinide Res. Commun.* **1986**, *1*, 195.
(11) Dai, S.; Toth, L. M.; Hayers, G. R.; Peterson, J. R. *Inorg. Chim. Acta* **1997**, *256*, 143.
(12) Dai, S.; Shin, Y. S.; Toth, L. M.; Barnes, C. E. *Inorg. Chem.* **1997**, *36*, 4900.
(13) Anderson, C. J.; Choppin, G. R.; Pruett, D. J.; Costa, D.; Smith, W. A. *Radiochim. Acta* **1999**, *84*, 31.
(14) Hopkins, T. A.; Berg, J. M.; Costa, D. A.; Smith, W. A.; Dewey, H. J. *Inorg. Chem.* **2001**, *40*, 1820.
(15) Costa, D. A.; Smith, W. H.; Dewey, H. J. *Proc. − Electrochem. Soc.* **2000**, *99−41* (Molten Salts XII).
(16) Schoebrechts, J. P.; Gilbert, B. *Inorg. Chem.* **1985**, *24*, 2105.
(17) Bhatt, A. I.; Dadds, B. L.; May, I.; Volkovich, V. A.; Charnock, J. M.; Bauer, A.; Hennig, C.; Rossberg, A. In *ROBL-CRG Bi-annual Report 2001/2002*; FZR-364; Schell, N., Ed., Project-Group ESRF-Beamline: Grenoble, France, 2003; p 109.
(18) Bhatt, A. I.; Kinoshita, H.; Koster, A. L.; May, I.; Sharrad, C. A.; Volkovich, V. A.; Fox, O. D.; Jones, C. J.; Lewin, B. G.; Charnock, J. M.; Hennig, C. *Proceedings ATALANTE 2004*; O13−04, Nimes, France, June 21−25, 2004.
(19) Nikitenko, S. I.; Moisy, P.; Berthon, C.; Bisel, I. *Proceedings ATALANTE 2004*; O25−05, Nimes, France, June 21−25, 2004.

Table 1. Voltammetric Parameters of the Fc^+/Fc Redox Couple at the GC Electrode in [BuMeIm][Tf_2N] and [$MeBu_3N$][Tf_2N] at 25 °C

ionic liquid	$E_{1/2}$ (V)	$(E_{pa} + E_{pc})/2$ (V)	ΔE_p (mV)	I_l at 1000 rpm (μA)
[BuMeIm][Tf_2N]	−0.387	−0.383	87	17.6
[$MeBu_3N$][Tf_2N]	−0.340	−0.343	225	4.1

prepared by immersing Ag wire in a 0.01 M solution of Ag(CF_3SO_3) in [BuMeIm][Tf_2N]. The reference solution was placed in a glass liquid junction protection tube with a fine porosity frit (from Radiometer). All potentials are reported with respect to this reference. The working electrode was polished on a damp cloth and washed in dioxane prior to use. The cell was deaerated with argon (O_2 < 0.1 ppm and H_2O < 0.5 ppm) for 30 min before the measurements. Argon was also sparged into the cell during the electrochemical data acquisition. The electrochemical measurements were performed at 25 ± 1 and 60 ± 1 °C. The temperature was controlled with a "Polystat 5" water thermostat. Preliminary voltammetric measurements were performed with 0.01 M solutions of ferrocene (Fc) in RTILs because the redox couple Fc^+/Fc is often used as an internal reference for electrochemical studies in nonaqueous solvents. The voltammetric parameters for the Fc^+/Fc couple are summarized in Table 1. The voltammetric half-wave potentials, measured from steady-state linear-sweep voltammograms, $E_{1/2}$, and from cyclic staircase voltammograms, $(E_{pa} + E_{pc})/2$, are independent of the electrode rotation rate, ω, and the potential scan rate, υ. The half-wave potential values are only about 45 mV more negative in [BuMeIm][Tf_2N] than in [$MeBu_3N$][Tf_2N], indicating the similarity of the Fc and Fc^+ species solvation in both ionic liquids. The peak potential separation, ΔE_p, considerably exceeds the theoretical value of 60 mV for a one-electron reversible electrode reaction. Furthermore, ΔE_p increases with the potential scan rate. These results indicate that the electrochemical oxidation of Fc involves a quasi-reversible charge-transfer process in the studied RTILs. The ΔE_p value in [$MeBu_3N$][Tf_2N] is almost two times larger and the limiting current, I_l, is approximately four times lower than in [BuMeIm][Tf_2N], most probably a result of the higher viscosity of [$MeBu_3N$][Tf_2N] (viscosities of [BuMeIm][Tf_2N] and [$MeBu_3N$][Tf_2N] are equal to 52 and 362 cP, respectively, at 25 °C).[1] It can be thus concluded that the relatively slow kinetics of Fc electrochemical oxidation is caused by the high viscosity of the ionic liquids.

Results and Discussion

1. Spectroscopic Analysis. The absorption spectra of [BuMeIm]$_2$[UCl_6] in [BuMeIm][Tf_2N], [$MeBu_3N$]$_2$[UCl_6] in [$MeBu_3N$][Tf_2N], and [BuMeIm]$_2$[UCl_6] in acetonitrile are illustrated in Figure 1. All the spectra present the same absorption maxima. The diffuse solid-state reflectance spectra of [BuMeIm]$_2$[UCl_6] and [$MeBu_3N$]$_2$[UCl_6], shown in Figure 2, agree closely with the absorption spectra of [cation]$_2$[UCl_6] in solutions. It is well-known that the U(IV)−hexachloro complex has a centrosymmetric octahedral arrangement in the solid state as well as in an acetonitrile solution.[20,21] Absorption bands have low intensities because electronic $f \rightarrow f$ transitions are Laport forbidden. It can be thus concluded that the octahedral anion UCl_6^{2-} is the predominant form of U(IV) in the solutions of [cation]$_2$[UCl_6] in Tf_2N^--based ionic liquids. Nevertheless, the intensities of the UCl_6^{2-} absorption bands are lower in acetonitrile than in RTILs. This can be attributed to the stronger solvation of UCl_6^{2-} in ionic liquids compared with that in acetonitrile.

Figure 3 demonstrates that the addition of water to 0.5 M has no significant effect on the absorption spectrum of [BuMeIm]$_2$[UCl_6] in [BuMeIm][Tf_2N], indicating the stability of UCl_6^{2-} with respect to hydrolysis in hydrophobic ionic liquids. The similar phenomenon observed recently for $NpCl_6^{2-}$ and $PuCl_6^{2-}$ in [BuMeIm][Tf_2N] was explained by the strong solvation of the $AnCl_6^{2-}$ anion in ionic liquids and by H-bonding of water molecules with Tf_2N^- anions.[19] Some differences in the peak intensities and in the structural details of the UCl_6^{2-} absorption spectra in a dried and hydrated ionic liquid can be attributed to a somewhat different solvation of the UCl_6^{2-} anions in these systems. Figure S1 (see Supporting Information) shows the UV/visible

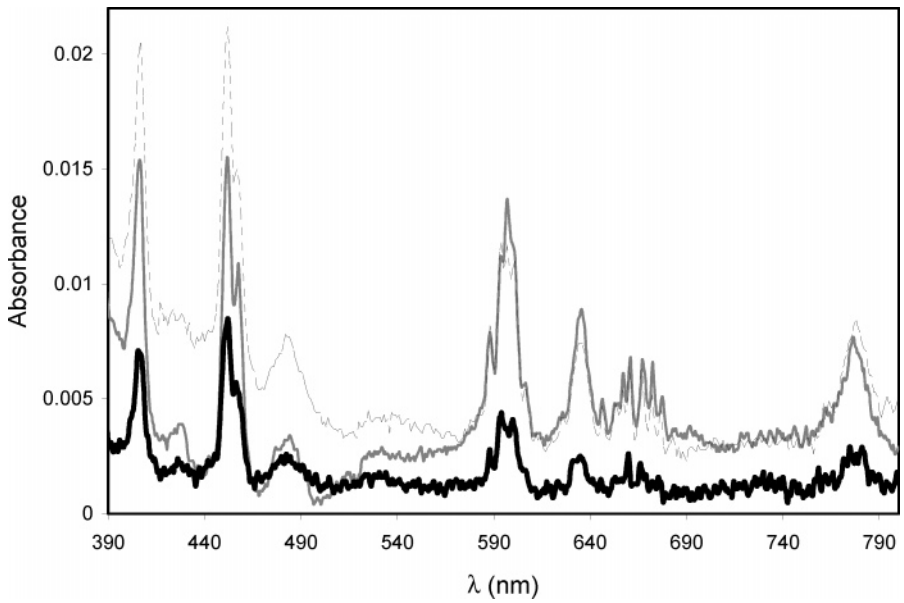

Figure 1. Absorption spectra of [BuMeIm]$_2$[UCl_6] (0.01 M) in [BuMeIm][Tf_2N] (solid gray line) and in acetonitrile (solid black line) and [$MeBu_3N$]$_2$-[UCl_6] (0.01 M) in [$MeBu_3N$][Tf_2N] (dotted line) at room temperature.

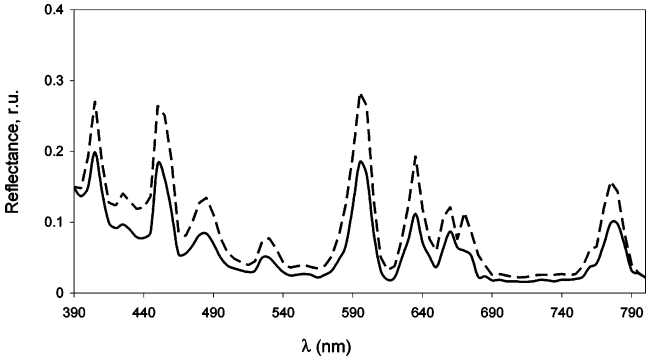

Figure 2. Diffuse solid-state reflectance spectra of $[BuMeIm]_2[UCl_6]$ (dashed line) and $[MeBu_3N]_2[UCl_6]$ (solid line).

spectrum of a UO_2Cl_2 solution in [BuMeIm][Tf_2N]. A comparison of the U(IV) and U(VI) spectra clearly indicate that the addition of water does not lead to any U(VI) oxidation.

2. Voltammetry of $[BuMeIm]_2[UCl_6]$ in [BuMeIm][Tf_2N]. The typical cyclic voltammograms of a neat [BuMeIm][Tf_2N] and a 0.01 M $[BuMeIm]_2[UCl_6]$ solution in [BuMeIm][Tf_2N] are shown in Figure 4, where it is clear that the electrochemical window of [BuMeIm][Tf_2N] spans the potential range from −2.5 to +1.0 V. The voltammogram of UCl_6^{2-} in this potential range reveals several electrochemical systems: (i) at $E_{p/2} = +0.27$ V (oxidation), (ii) at $E_{p/2} = -1.96$ V (reduction I), and (iii) at $E_{pc} = -1.4$ V and $E_{pa} = -0.4$ V (reduction II). The peak currents for the oxidation and the reduction I processes have comparable intensities. By contrast, the peak intensity of the reduction II process is much lower. Each process is examined separately.

2.1. Oxidation. Steady-state linear-sweep voltammograms of U(IV), recorded in the potential range from 0 to +0.6 V (Figure 5), exhibit one anodic wave related to U(IV) electrochemical oxidation. The cyclic staircase voltammograms for the U(IV) oxidation process are shown in Figure S2 (see Supporting Information). The cyclic voltammetry parameters for the oxidation process are presented in Table 2. The peak current ratio I_{pc}/I_{pa} increases and approaches 1 as the potential scan rate increases, indicating the relatively low stability of the oxidized uranium species. A variation of ΔE_p with v and the linear plot of I_{pa} and I_{pc} with $v^{1/2}$ demonstrate that the process is quasi-reversible. One can conclude that the U(IV) oxidation occurs without a chloride-ion transfer. This redox couple could thus correspond to a one-electron exchange system, UCl_6^-/UCl_6^{2-}, according to eq 1.

$$UCl_6^{2-} \rightarrow UCl_6^- + e^- \quad (1)$$

2.2. Reduction I. Voltammetric parameters for the redox couple at $E_{p/2} = -1.96$ V are presented in Table 3 , and the corresponding cyclic voltammograms are reported in Figure S3 (see Supporting Information). The resemblance of this process with the UCl_6^{2-} one-electron electrochemical reduction in chloroaluminate-based ionic liquids[9,15] suggests that the system at $E_{p/2} = -1.96$ V corresponds to the reduction of U(IV) to U(III) without chloride-ion transfer (eq 2).

$$UCl_6^{2-} + e^- \rightarrow UCl_6^{3-} \quad (2)$$

The I_{pa}/I_{pc} ratio is independent of the potential scan rate and close to 1, indicating the relative stability of UCl_6^{3-} in [BuMeIm][Tf_2N].

2.3. Reduction II. The voltammograms in Figure 6 demonstrate a reduction peak, IIc, at −1.4 V and an oxidation peak, IIa1, at −0.4 V, with a shoulder, IIa2, at −0.73 V in the 0 to −1.6 V potential region at a 100 mV s^{-1} scan rate. However, if the potential is scanned first in the positive direction (dashed curve), no oxidation peak is observed. So, the processes observed at −0.73 and −0.4 V would correspond to the oxidation of the species formed after reduction at −1.4 V. The reduction II process is thus irreversible. Cyclic voltammograms corresponding to this process as a function of the scan rate are reported in Figure S4 (see Supporting Information), and the I_p and E_p values are reported in Table 4. The $I_{pa}(-0.4\text{ V})/I_{pc}(-1.4\text{ V})$ ratio decreases when the potential scan rate increases.

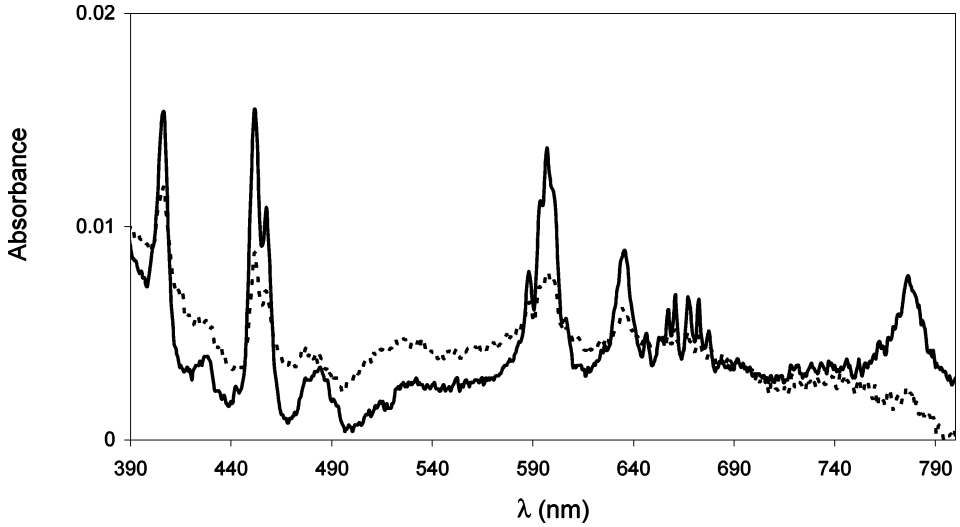

Figure 3. Absorption spectra of $[BuMeIm]_2[UCl_6]$ (0.01 M) in dried [BuMeIm][Tf_2N] (solid line) and in the presence of 0.5 M H_2O (dashed line) at room temperature.

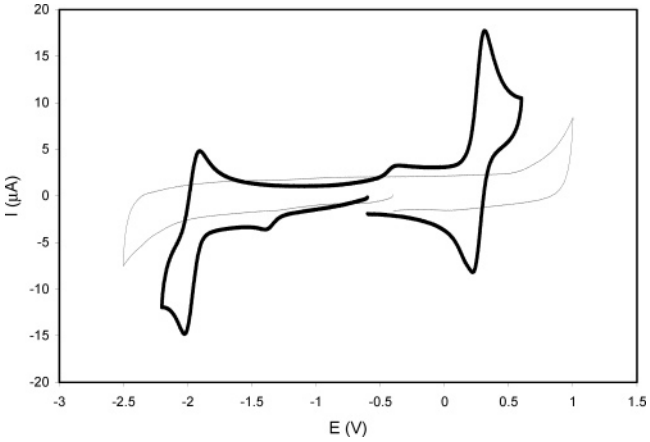

Figure 4. Cyclic voltammograms of [BuMeIm][Tf_2N] alone (grey line) and in the presence of 0.01 M [BuMeIm]$_2$[UCl_6] (solid line). $v = 100$ mV s^{-1}, $T = 25$ °C, and the GC electrode area 0.07 = cm^2. $E_i = -0.4$ V, $E_{inv1} = -2.5$ V, $E_{inv2} = 1$ V, and $E_f = -0.4$ V (dashed curve); $E_i = -0.6$ V, $E_{inv1} = -2.2$ V, $E_{inv2} = 0.6$ V, and $E_f = -0.6$ V (solid curve).

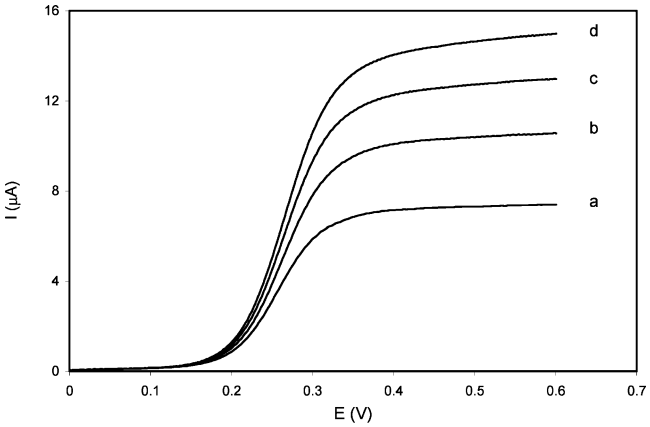

Figure 5. Steady-state linear-sweep voltammograms of 0.01 M [BuMeIm]$_2$-[UCl_6] in [BuMeIm][Tf_2N] at 500 (a), 1000 (b), 1500 (c), and 2000 rpm (d). $v = 5$ mV s^{-1}, $T = 25$ °C, and the GC electrode area = 0.07 cm^2. $E_i = 0$ V and $E_f = 0.6$ V.

Table 2. Dependence of Peak Potentials and Peak Intensities on the Potential Scan Rate at 25 °C for the Oxidation I Process of [BuMeIm]$_2$[UCl_6] in [BuMeIm][Tf_2N]

v (mV s^{-1})	25	50	100	150	200
E_{pa} (V)	0.31	0.31	0.315	0.32	0.32
E_{pc} (V)	0.21	0.22	0.22	0.22	0.22
ΔE_p (mV)	100	90	95	100	100
$(E_{pa} + E_{pc})/2$ (V)	0.26	0.26	0.27	0.27	0.27
I_{pa} (μA)	7.5	10.4	15	17.9	20.8
$-I_{pc}$ (μA)	4.6	8.3	13.3	15.4	18.7
$\lvert I_{pc}/I_{pa}\rvert$	0.61	0.8	0.89	0.86	0.9

For the reduction II process, we could thus propose the mechanism of the UCl_6^{2-} reduction followed by the rearrangement of the UCl_6^{3-} coordination environment as a result of the coordination of U(III) with Tf_2N^-, according to eqs 3 and 4.

$$UCl_6^{2-} + e^- \rightarrow UCl_6^{3-} \quad (3)$$

$$UCl_6^{3-} + xTf_2N^- \rightarrow UCl_6(Tf_2N)_x^{-(3+x)} \quad (4)$$

The Tf_2N^- anion is known to be a weak ligand exhibiting oxygen coordination as η^1-O or η^2-O,O to actinides or lanthanides.[22] This ligand is not able to replace the Cl^- anion from the coordination octahedron of UCl_6^{2-}. However, the stability of $AnCl_6^{3-}$ complexes in general is lower than that of $AnCl_6^{2-}$.[23] The Tf_2N^- anion concentration is much higher than that of chloride in solutions of 0.01 M [BuMeIm]$_2$[UCl_6] in ionic liquids. For example, the concentration of the Tf_2N^- anion is 3.5 M in neat [BuMeIm][Tf_2N]. One can conclude that at least part of the U(III) hexachloride can be transformed to the $UCl_6(Tf_2N)_x^{-(3+x)}$ complex as a result of the Tf_2N^--ligand coordination with U(III). The peak currents for the reduction II process are much lower than for the reduction I process, indicating the relatively low yield of the U(III) mixed-ligand species.

Table 3. Dependence of Peak Potentials and Peak Intensities on the Potential Scan Rate at 25 °C for the Reduction I Process of [BuMeIm]$_2$[UCl_6] in [BuMeIm][Tf_2N]

v (mV s^{-1})	25	50	100	150	200
E_{pa} (V)	−1.9	−1.9	−1.9	−1.9	−1.9
E_{pc} (V)	−2.01	−2.02	−2.02	−2.03	−2.04
ΔE_p (mV)	110	120	120	130	140
$(E_{pa} + E_{pc})/2$ (V)	−1.95	−1.96	−1.96	−1.96	−1.97
I_{pa} (μA)	3.8	6.5	9.1	11.5	13.2
$-I_{pc}$ (μA)	5.3	7.9	12.3	13.8	15.9
$\lvert I_{pa}/I_{pc}\rvert$	0.72	0.82	0.74	0.83	0.83

Table 4. Dependence of Peak Potentials and Peak Intensities on the Potential Scan Rate at 25 °C for the Reduction II Process of [BuMeIm]$_2$[UCl_6] in [BuMeIm][Tf_2N] at −1.4 V/−0.4 V

v (mV s^{-1})	10	25	100	200
E_{pc} (V)	−1.39	−1.39	−1.405	−1.41
$-I_{pc}$ (μA)	0.52	0.74	1.5	1.92
E_{pa} (V)	−0.46	−0.46	−0.45	−0.43
I_{pa} (μA)	0.3	0.37	0.44	0.6
$\lvert I_{pa}/I_{pc}\rvert$	0.58	0.5	0.29	0.31

Figure 7A shows the steady-state linear-sweep voltammograms recorded in the negative potential direction at different electrode rotation rates. At $\omega = 1000$ rpm, a cathodic wave is observed at $E_{1/2} = -1.4$ V and at $E_{1/2} = -2.0$ V, corresponding to the second and first reduction processes of UCl_6^{2-}, respectively. However, according to the cyclic voltammetry analysis, the intensity of the reduction wave at $E_{1/2} = -2.0$ V should be greater than that at $E_{1/2} = -1.4$ V. Moreover, if the rotation rate is increased to 1500 rpm, the cathodic wave at $E_{1/2} = -2.0$ V is no longer detectable. We can thus assume that the redox process at $E_{1/2} = -1.4$ V involves the precipitation of the presumed $UCl_6(Tf_2N)_x^{-(3+x)}$ complexes at the electrode surface. Increasing the electrode rotation rate increases the reduced-chemical-form yield followed by passivation of the electrode. Figure 7B demonstrates the steady-state linear-sweep voltammograms recorded at the same electrode rotation rate (1000 rpm) but at different initial potentials. The scan in the potential range from −1.0 to −2.2 V exhibits only one reduction wave at $E_{1/2} = -1.4$ V (reduction II). However, if the scan begins at −1.7 V, the cathodic wave of reduction I

(20) Siegel, A. *Acta Crystallogr.* **1956**, *9*, 827.
(21) Gans, P.; Hathaway, B. J.; Smith, B. C. *Spectrochim. Acta* **1965**, *21*, 1589.
(22) Williams, D. B.; Stoll, M. E.; Scott, B. L.; Costa, D. A.; Oldham, W. I. *Chem. Commun.* **2005**, *11*, 1438.
(23) Barbanel, A. Y. *J. Inorg. Nucl. Chem.* **1976**, 79 (supplementary volume).

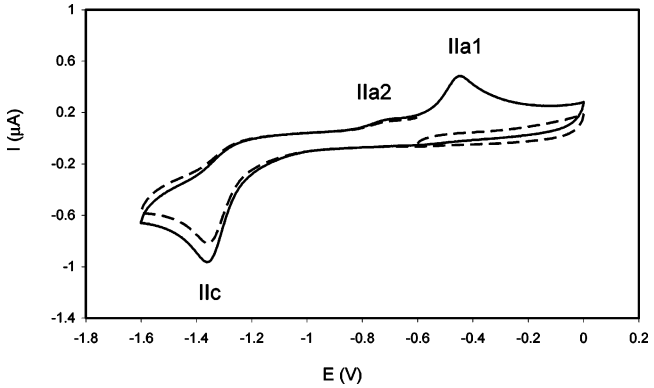

Figure 6. Cyclic voltammograms of 0.01 M $[BuMeIm]_2[UCl_6]$ in $[BuMeIm][Tf_2N]$. $v = 100$ mV s^{-1}, $T = 25$ °C, and the GC electrode area $= 0.07$ cm^2. $E_i = -0.6$ V, $E_{inv1} = 0$ V, $E_{inv2} = -1.6$ V, and $E_f = -0.6$ V (dashed curve); $E_i = -0.7$ V, $E_{inv1} = -1.6$ V, $E_{inv2} = 0$ V, and $E_f = -0.7$ V (solid curve).

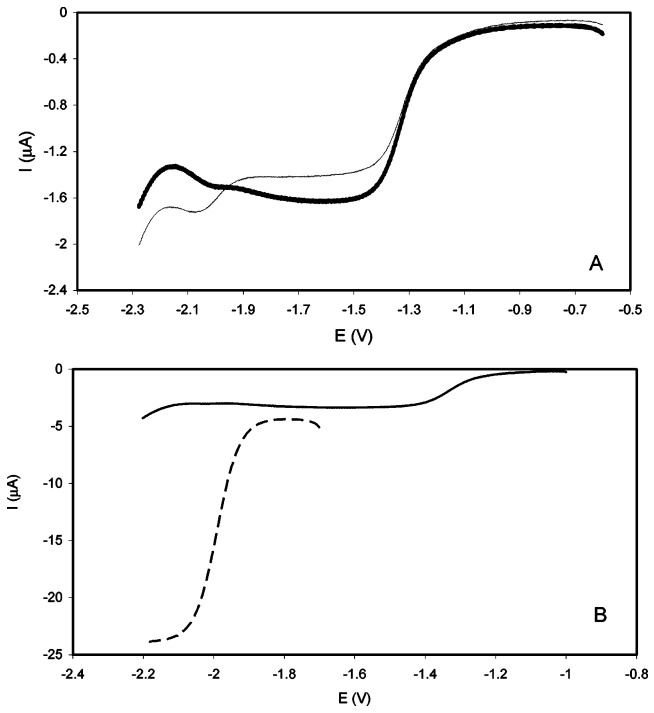

Figure 7. Steady-state linear-sweep voltammograms of 0.01 M $[BuMeIm]_2[UCl_6]$ in $[BuMeIm][Tf_2N]$. $v = 5$ mV s^{-1}, $T = 25$ °C (A) and 60 °C (B), and the GC electrode area $= 0.07$ cm^2. (A) $\omega = 1000$ rpm (grey line) and 1500 rpm (black line). $E_i = -0.6$ V and $E_f = -2.3$ V. (B) $\omega = 1000$ rpm. $E_i = -1$ V and $E_f = -2.2$ V (solid line); $E_i = -1.7$ V and $E_f = -2.2$ V (dashed line).

is clearly observed at $E_{1/2} = -2.0$ V. This observation confirms the hypothesis about electrode passivation during the reduction II process.

In principle, other hypotheses could be proposed concerning the uranium chemical form obtained by the reduction II process:

(I) Reduction II could be related to some hydrolyzed form of U(IV). However, the absorption spectrum of a 0.01 M $[BuMeIm]_2[UCl_6]$ solution in $[BuMeIm][Tf_2N]$ with water to a total concentration of 0.5 M shows the same absorption maxima as does the absorption spectrum without water. The hexachloro complex seems to be stable with respect to hydrolysis in $[BuMeIm][Tf_2N]$. Moreover, it is usually hard to reduce the hydrolyzed U(IV) form to U(III). The process

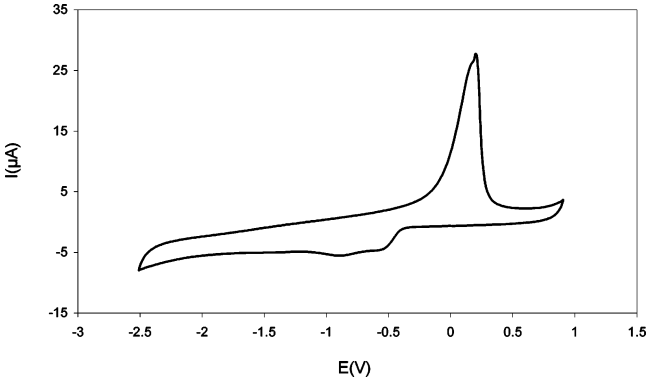

Figure 8. Cyclic voltammogram of 0.01 M UO_2Cl_2 in $[BuMeIm][Tf_2N]$. $v = 100$ mV s^{-1}, $T = 25$ °C, and the GC electrode area $= 0.07$ cm^2. $E_i = 0$ V, $E_{inv1} = -2.5$ V, $E_{inv2} = 0.9$ V, and $E_f = 0$ V.

at -1.4 V should thus not be related to the reduction of the U(IV) hydrolyzed form.

(II) Process II would represent the reduction of UO_2^{2+} produced by the oxidation of U(IV) in the presence of traces of oxygen. The cathodic process observed at -1.4 V should thus be attributed to the U(VI)/U(IV) reduction followed by adsorption of the U(IV) oxo species on the electrode. However, the absorption spectrum of a $[BuMeIm]_2[UCl_6]$ solution in $[BuMeIm][Tf_2N]$ does not exhibit any absorption band specific to the uranyl species. The absorption spectrum of a UO_2Cl_2 solution in $[BuMeIm][Tf_2N]$, shown in Figure S1 (see Supporting Information), indicates that UO_2^{2+} should be detected, even for a concentration of 10^{-3} M (that is 10% of the total uranium concentration). Figure 8 shows the cyclic voltammogram of a UO_2Cl_2 solution in $[BuMeIm][Tf_2N]$. Two poorly resolved cathodic waves at -0.60 and -0.95 V (100 mV s^{-1}) can be attributed to UO_2^{2+} electrochemical reduction followed by the formation of U(IV) oxo complexes adsorbed at the electrode surface. The sharp anodic peak at $+0.21$ V (100 mV s^{-1}) should be thus related to the reoxidation of U(IV). The reduction peak potentials of UO_2^{2+} are quite different from the reduction peak potentials of the reduction II process. So, we have concluded that process II does not correspond to UO_2^{2+} reduction.

Finally, the hypothesis about the formation of a mixed-ligand complex, $UCl_6(Tf_2N)_x^{-(3+x)}$, appears more attractive than the others. However, additional investigation is needed to confirm this assumption.

3. Voltammetry of $[MeBu_3N]_2[UCl_6]$ in $[MeBu_3N][Tf_2N]$. The cyclic voltammogram in Figure 9A demonstrates that the electrochemical window of dried $[MeBu_3N][Tf_2N]$ is still larger than that of $[BuMeIm][Tf_2N]$ and spans from -3.5 to $+1.0$ V at the GC electrode in the presence of Ar. Adding metallic sodium to dried $[MeBu_3N][Tf_2N]$ does not lead to any change in the solvent, even under gentle heating. By contrast, the color of dried $[BuMeIm][Tf_2N]$ turns dark brown in the presence of metallic sodium, even at room temperature. It can be concluded that the reduction potentials of $MeBu_3N^+$ and $BuMeIm^+$ cations are more negative and more positive, respectively, than the reduction potential of the Na^+ cation equal to -2.71 V versus a normal hydrogen electrode (NHE) in an aqueous solution.

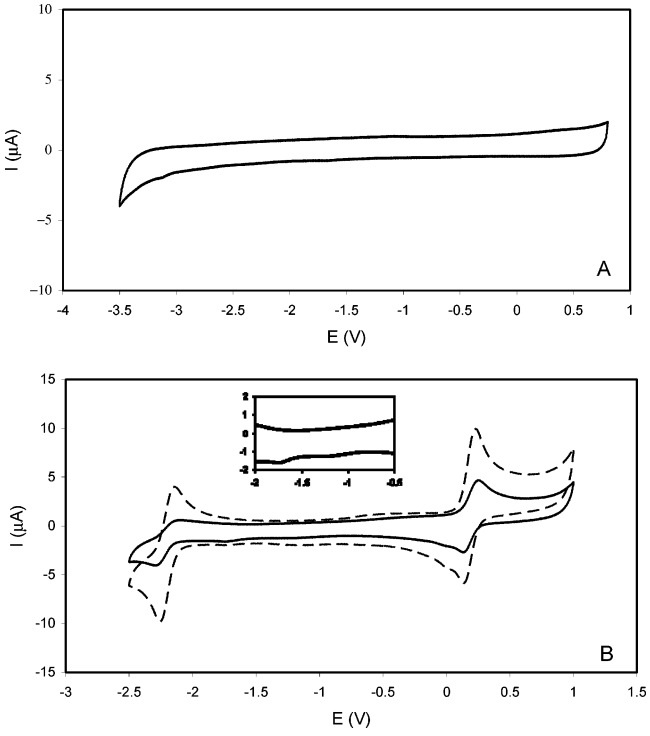

Figure 9. Cyclic voltammograms of dried $[MeBu_3N][Tf_2N]$ alone (A) and in the presence of 0.01 M $[MeBu_3N]_2[UCl_6]$ (B). $\upsilon = 100$ mV s^{-1}, $T = 25$ °C (solid line) and 60 °C (dashed line), and the GC electrode area = 0.07 cm^2. (A) $E_i = 0$ V, $E_{inv1} = -3.5$ V, $E_{inv2} = 0.8$ V, and $E_f = 0$ V. (B) $E_i = -0.5$ V, $E_{inv1} = -2.5$ V, $E_{inv2} = 1$ V, and $E_f = -0.5$ V.

The cyclic voltammogram of $[MeBu_3N]_2[UCl_6]$ in $[MeBu_3N][Tf_2N]$ scanned in the potential range of −2.7 to +0.8 V (Figure 9B) reveals two redox systems with comparable intensities at +0.19 and −2.2 V, which can be attributed to the oxidation and reduction I processes, respectively. A reduction peak at −1.75 V and a shoulder at −1.55 V can be observed, but they have very low intensities (see inset in Figure 9B). At the reverse scan, no oxidation peak is related to the reduction processes at −1.55 or −1.75 V. These minor processes could be attributed to the reduction II reaction observed in $[BuMeIm][Tf_2N]$. In general, UCl_6^{2-} exhibits the same redox behavior in $[MeBu_3N][Tf_2N]$ and in $[BuMeIm][Tf_2N]$. However, the peak intensities in $[MeBu_3N][Tf_2N]$ are much lower than the peak intensities in $[BuMeIm][Tf_2N]$ as a result of the higher viscosity of the tetraalkyl-based ionic liquid. Raising the temperature to 60 °C causes a severalfold increase in the peak intensities, reflecting an increase in the rate of mass transport. The differences between the anodic and the cathodic peak potentials are also smaller at 60 °C than those at 25 °C; therefore, the systems are better defined. We will consider only the redox couples at +0.19 and −2.2 V because the peak currents of the third process are too small to be analyzed correctly.

3.1. Oxidation at +0.19 V. The steady-state linear-sweep voltammogram of the UCl_6^{2-} electrochemical oxidation is shown in Figure 10. Uranium(IV) exhibits only one anodic wave in $[MeBu_3N][Tf_2N]$ similar to that observed in $[BuMeIm][Tf_2N]$. Contrary to $[BuMeIm][Tf_2N]$ solutions, the linear-sweep voltammograms recorded in $[MeBu_3N][Tf_2N]$,

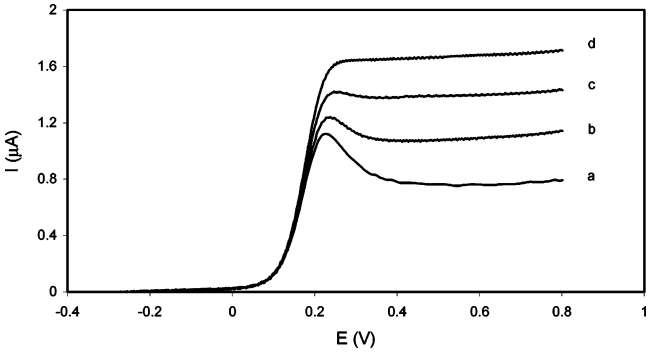

Figure 10. Steady-state linear-sweep voltammograms of 0.01 M $[MeBu_3N]_2[UCl_6]$ in $[MeBu_3N][Tf_2N]$ at 500 (a), 1000 (b), 1500 (c), and 2000 rpm (d). $\upsilon = 5$ mV s^{-1}, $T = 25$ °C, and the GC electrode area = 0.07 cm^2. $E_i = -0.3$ V and $E_f = 0.8$ V.

Table 5. Dependence of Peak Potentials and Peak Intensities on the Potential Scan Rate at 25 °C for the Oxidation I Process of $[MeBu_3N]_2[UCl_6]$ in $[MeBu_3N][Tf_2N]$

υ (mV s^{-1})	10	25	50	100	150	200
E_{pa} (V)	0.235	0.24	0.25	0.255	0.265	0.27
E_{pc} (V)	0.135	0.132	0.135	0.125	0.12	0.115
ΔE_p (mV)	100	108	115	130	145	155
$(E_{pa} + E_{pc})/2$ (V)	0.185	0.186	0.19	0.19	0.19	0.19
I_{pa} (μA)	1	1.77	2.66	3.55	4.22	5.17
$-I_{pc}$ (μA)	0.61	1.33	2.11	3	3.9	4.44
$\lvert I_{pc}/I_{pa}\rvert$	0.61	0.75	0.79	0.84	0.92	0.86

Table 6. Dependence of Peak Potentials and Peak Intensities on the Potential Scan Rate at 25 °C for the Reduction I Process of $[MeBu_3N]_2[UCl_6]$ in $[MeBu_3N][Tf_2N]$

υ (mV s^{-1})	25	50	100	150	200
E_{pa} (V)	−2.1	−2.1	−2.09	−2.08	−2.08
E_{pc} (V)	−2.3	−2.3	−2.3	−2.3	−2.31
ΔE_p (mV)	200	200	210	220	230
$(E_{pa} + E_{pc})/2$ (V)	−2.2	−2.2	−2.2	−2.19	−2.2
I_{pa} (μA)	0.66	1	1.33	1.67	1.83
$-I_{pc}$ (μA)	1.22	1.8	2.5	2.78	3.1
$\lvert I_{pa}/I_{pc}\rvert$	0.54	0.55	0.53	0.6	0.59

at a relatively low electrode rotation speed, do not show a current plateau but instead show some current maximum. This phenomenon, already described for RTILs,[1] is related to the high viscosity of the ionic liquids when the steady state cannot be reached at a low rotation speed. Table 5 summarizes the voltammetric parameters for reaction 1 in $[MeBu_3N][Tf_2N]$ at 25 °C, determined from cyclic voltammograms reported in Figure S5 (see Supporting Information). The variation of ΔE_p with υ and the linear plots of I_{pa} and I_{pc} with $\upsilon^{1/2}$ suggest that the redox system UCl_6^{-}/UCl_6^{2-} is quasi-reversible, similar to that in $[BuMeIm][Tf_2N]$. The voltammetric half-wave potential of the U(V)/U(IV) couple in $[MeBu_3N][Tf_2N]$ is 80 mV more negative than in $[BuMeIm][Tf_2N]$. This difference is greater than in the case of Fc oxidation in both ionic liquids (Table 1), probably as a result of the fact that Fc is a neutral molecule that weakly interacts with the solvent.

3.2. Reduction at −2.2 V. Voltammetric data on reduction I in $[MeBu_3N][Tf_2N]$ are shown in Table 6 and are measured from cyclic voltammograms reported in Figure S6 (see Supporting Information). Analyses of the variation of ΔE_p with υ and the peak currents with $\upsilon^{1/2}$ indicate that reaction 2 is quasi-reversible in $[MeBu_3N][Tf_2N]$ as well as in $[BuMeIm][Tf_2N]$. In $[MeBu_3N][Tf_2N]$, the half-wave poten-

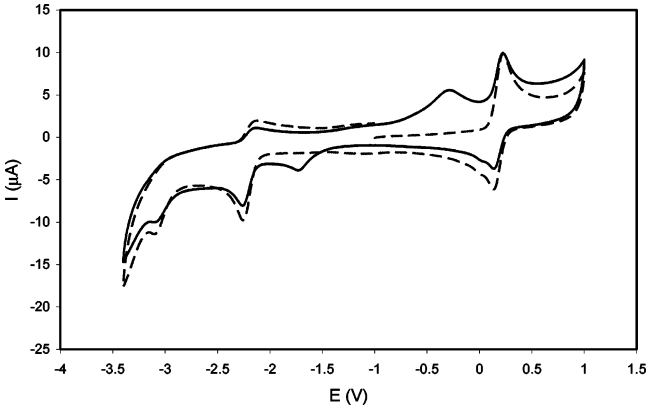

Figure 11. Cyclic voltammograms of 0.01 M $[MeBu_3N]_2[UCl_6]$ in $[MeBu_3N][Tf_2N]$ at the first scan (dashed line) and the third scan (solid line). $\upsilon = 100$ mV s^{-1}, $T = 60$ °C, and the GC electrode area = 0.07 cm^2. $E_i = -1$ V, $E_{inv1} = 1$ V, $E_{inv2} = -3.4$ V, and $E_f = -1$ V.

tial of the UCl_6^{2-}/UCl_6^{3-} couple is shifted almost 250 mV negatively compared with the potential in $[BuMeIm][Tf_2N]$. This difference is most probably related to the effect of the ionic liquid cation on the anionic complexes of uranium at different oxidation states. Electrochemical studies of anionic complexes for various transition metals in chloroaluminate ionic liquids revealed the strong solvation of anionic species in RTILs via the formation of ion pairs.[24] The effect of ion pairing on the UCl_6^{2-}/UCl_6^{3-} redox couple would be more significant than on the UCl_6^{-}/UCl_6^{2-} couple because the overall negative charge of UCl_6^{3-} is higher than that of UCl_6^{-}. It can be thus concluded that $BuMeIm^+$ interacts more strongly with uranium anionic complexes than with $MeBu_3N^+$. The theoretical molecular dynamics study has shown that the $EuCl_6^{3-}$ complex in the ionic liquid $[BuMeIm][PF_6]$ is embedded in a shell of $BuMeIm^+$ cations whose C_2H, C_4H, and C_5H aromatic protons are hydrogen-bonded to the Cl^- ligands of the complex.[25] The energy of hydrogen bonding is obviously lower for the aliphatic protons of the $MeBu_3N^+$ cation.

3.3. Redox Behavior in the Potential Range of −3.5 to +1 V. The high cathodic stability of $[MeBu_3N][Tf_2N]$ allows the electrochemical behavior of metal complexes to be studied to −3.5 V. For example, electrochemical reduction of Cs^+ ($E = -2.923$ V vs NHE)[26] has been recently reported in $[MeBu_3N][Tf_2N]$ at −3.6 and −2.3 V versus Fc^+/Fc at W and Hg working electrodes, respectively.[27] Figure 11 shows the cyclic voltammograms of UCl_6^{2-} in $[MeBu_3N]$-$[Tf_2N]$ in the potential range of −3.5 to +1 V. A third cathodic wave is seen clearly at $E_p = -3.12$ V (100 mV s^{-1}). Moreover, a voltammogram recorded to the positive potential after the reduction at −3.12 V exhibits a reoxidation process at −0.16 V, and coupled with it is a cathodic wave at −1.77 V. The irreversible redox system at potentials of −0.16 V/−1.77 V closely resembles the reduction II process, which is presumably related to the formation of mixed-ligand complexes $UCl_6(Tf_2N)_x^{-(3+x)}$.

The peak potential of the third cathodic wave is shifted negatively by more than 1 V compared with that of the UCl_6^{2-}/UCl_6^{3-} reduction potential. It appears relatively unlikely that this process is related to any U(IV)/U(III) reduction. Taking into account that the standard U(III)/U(0) redox potential is estimated to be −2.6 V versus Ag/Ag(I) in aqueous solution,[26] the reduction wave at −3.12 V can be attributed to the reduction of U(III) to U(0). In this case, the anodic wave at −0.16 V should correspond to the electrochemical redissolution of metallic uranium, followed by the formation of U(IV) complexes. The reason for the dramatic difference between the potential of the U(III) reduction and the potential of the U(0) reoxidation is unclear. It can be assumed that the electrochemical redissolution of U(0) is accompanied by a complexation with Cl^- or Tf_2N^- anions. The complexation processes are usually very slow in viscous RTILs. The slow kinetics gives rise to the overvoltage of the U(0) redissolution. Another explanation of the abnormal uranium redissolution behavior can be related to the instability of the finely divided metallic uranium, which can react with traces of water or oxygen in RTIL giving oxo or hydroxo species of U(IV) at the electrode surface. However, the reoxidation peak potential is 0.36 V more positive than that found for the U(IV) oxo species oxidation in a solution of UO_2Cl_2 (Figure 8). We can conclude that the reoxidation peak at −0.16 V is not related to the oxidation of U(IV) oxo species. Indeed, additional investigations are necessary to establish the nature of the uranium reduction processes in hydrophobic RTILs.

Conclusions

The absorption spectra of $[cation]_2[UCl_6]$, where $[cation]^+$ is $[BuMeIm]^+$ and $[MeBu_3N]^+$, in solutions of hydrophobic ionic liquids $[BuMeIm][Tf_2N]$ and $[MeBu_3N][Tf_2N]$ are similar to the diffuse solid-state reflectance spectra of the corresponding solid complexes, indicating that the octahedral complex UCl_6^{2-} is the predominant chemical form of U(IV) in Tf_2N^--based RTILs.

The spectroscopic study has also shown that the hexachloro complexes of U(IV) are stable with respect to hydrolysis in the studied hydrophobic ionic liquids.

The electrochemical window of RTILs spans the potential range of −2.5 to +1.0 V for $[BuMeIm][Tf_2N]$ and −3.5 to +1.0 V for $[MeBu_3N][Tf_2N]$ at the GC working electrode. This large electrochemical window allowed the study for the first time of both reduction and oxidation of UCl_6^{2-} in the same experimental conditions.

Voltammograms of UCl_6^{2-} in both RTILs over the potential range of −2.5 to +1.0 V reveal several electrochemical systems attributed to the following processes:

$$UCl_6^{2-} \rightarrow UCl_6^{-} + e^-$$

$$UCl_6^{2-} + e^- \rightarrow UCl_6^{3-}$$

$$UCl_6^{2-} + e^- + xTf_2N^- \rightarrow UCl_6(Tf_2N)_x^{-(3+x)}$$

(24) Hussey, C. L.; Sun, I.-W.; Strubinger, S. K. D.; Barnard, P. A. *J. Electrochem. Soc.* **1990**, *137*, 2515.
(25) Chaumont, A.; Wipff, G. *Inorg. Chem.* **2004**, *43*, 5891.
(26) *Handbook of Chemistry and Physics*, 49th edition; Weast, R. C., Ed.; The Chemical Rubber Co.: Cleveland, OH, 1986.
(27) Chen, P.-Y.; Hussey, C. L. *Electrochim. Acta* **2004**, *49*, 5125.

Even in the absence of chloride ions in the solution, the electrochemical study has shown the relative stability of the hexachloro−uranium complexes, UCl_6^- and UCl_6^{3-}.

Our data clearly show that uranium redox potential values depend strongly on the RTIL cation. Moreover, the U(IV)/U(III) redox couple is more sensitive to the RTIL cation than is the U(V)/U(IV) couple, as the half-wave potential of the U(V)/U(IV) couple is 80 mV and that of the U(IV)/U(III) couple is 250 mV more positive in [BuMeIm][Tf_2N] than in [$MeBu_3N$][Tf_2N]. This was attributed to the difference in solvation of the uranium complexes in the two ionic liquids. These new fundamental data indicate that the hydrophobic ionic liquids cannot be considered as inert solvents with respect to An(IV)−hexachloro complexes.

Scanning the negative potential to −3.5 V in [$MeBu_3N$][Tf_2N] solutions of UCl_6^{2-} reveals the presence of an irreversible cathodic process at the peak potential equal to −3.12 V at 100 mV s^{-1} and 60 °C. This cathodic wave could be attributed to the reduction of U(III) to U(0).

Acknowledgment. This work was supported by the European ACTINET network and GDR Paris (French organization).

Supporting Information Available: Absorption spectra of a 0.01 M [BuMeIm]$_2$[UCl_6] and a 0.01 M UO_2Cl_2 solution in [BuMeIm][Tf_2N] at room temperature. Cyclic voltammograms of 0.01 M [BuMeIm]$_2$[UCl_6] in [BuMeIm][Tf_2N] as a function of the potential scan rate for the oxidation, reduction I, and reduction II processes and of 0.01 M [$MeBu_3N$][UCl_6] in [$MeBu_3N$][Tf_2N] as a function of the potential scan rate for the oxidation and reduction I processes. This material is available free of charge via the Internet at http://pubs.acs.org.

IC051065B